

New companions in the stellar systems of DI Cha, Sz 22, CHXR 32, and Cha H α 5 in the Cha I star-forming region \star

T. O. B. Schmidt¹, N. Vogt², R. Neuhäuser¹, A. Bedalov^{1,3}, and T. Roell¹

¹ Astrophysikalisches Institut und Universitäts-Sternwarte, Universität Jena, Schillergäßchen 2-3, 07745 Jena, Germany
e-mail: tobi@astro.uni-jena.de

² Departamento de Física y Astronomía, Universidad de Valparaíso, Avenida Gran Bretaña 1111, Valparaíso, Chile

³ Faculty of Natural Sciences, University of Split, Teslina 12. 21000 Split, Croatia

Received 2012; accepted

ABSTRACT

Context. The star-forming regions in Chamaeleon (Cha) are among the nearest (distance ~ 165 pc) and youngest (age ~ 2 Myrs) conglomerates of recently formed stars and among the ideal targets for studies of star formation.

Aims. We search for new, hitherto unknown binary or multiple-star components and investigate their membership in Cha and their gravitationally bound nature.

Methods. We used the Naos-Conica (NACO) instrument at the Very Large Telescope Unit 4/YEPUN of the Paranal Observatory, at 2 or 3 different epochs, in order to obtain relative and absolute astrometric measurements, as well as differential photometry in the J, H, and Ks band. On the basis of known proper motions and these observations, we analysed the astrometric results in our proper motion diagrams (PMD: angular separation / position angle versus time) to eliminate possible (non-moving) background stars and establish co-moving binaries and multiples.

Results. DI Cha turns out to be a quadruple system with a hierarchical structure, consisting of two binaries: a G2/M6 pair and a co-moving pair of two M5.5 dwarfs. For both pairs we detected orbital motion ($P \sim 130$ and ~ 65 years respectively), although in opposite directions. Sz 22 is a binary whose main component is embedded in a circumstellar disc or reflection nebula, accompanied by a co-moving M4.5 dwarf. CHXR 32 is a triple system, consisting of a single G5 star, weakened by an edge-on disc and a co-moving pair of M1/M3.5 dwarfs whose components show significant variations in their angular separation. Finally, Cha H α 5 is a binary consisting of two unresolved M6.5 dwarfs whose strong variations in position angle at its projected separation of only 8 AU imply an orbital period of ~ 46 years. DI Cha D and Cha H α 5 A & B are right at the stellar mass limit and could possibly be brown dwarfs.

Conclusions. In spite of various previously published studies of the star-forming regions in Cha we still found four hitherto unknown components in young low-mass binaries and multiple systems. All are gravitationally bound, and at least the case Cha H α 5 presents a link between our high-resolution astrometry and the radial velocity method, avoiding a blind gap of detection possibility.

Key words. Stars: imaging, pre-main sequence, binaries: visual, brown dwarfs – Astrometry – Infrared: stars – Protoplanetary discs

1. Introduction

The star-forming region Cha I (Luhman 2008) is rather close to the Sun (distance ~ 165 pc) and is young (age ~ 2 Myrs), among the ideal targets for population studies of young stars, brown dwarfs, and planetary bodies. In this context, the occurrence and properties of binaries and multiple systems can play a key role in understanding the underlying physical processes in the formation and evolution of recently formed stars and their companions. Our working group is carrying out a long-term programme, obtaining astrometry and differential photometry in the near-infrared JHKs bands from images at the Very Large Telescope (VLT at Paranal Observatory of the European Southern Observatory, ESO), Unit Telescope (UT) 4 (Yepun) with Naos-Conica (NACO, Lenzen et al. 2003; Rousset et al.

2003) at different epochs. First results of this campaign have been published by Schmidt et al. (2008a,b) and by Vogt et al. (2012, hereafter Paper I). The latter paper confirms 16 gravitationally bound binaries or multiple systems in the star-forming regions in Cha. The purpose of the present paper is to complement this information, presenting and confirming new faint companions in a total of four stellar systems, all members of the star-forming region Cha I.

In Section 2 we describe our observations, as well as the background star density and its relation to the interstellar extinction in the surroundings of our targets. In Section 3 we present the individual target stars in detail, based on their images reproduced from our NACO fields and the corresponding proper motion diagrams (PMDs). Section 4 contains concluding remarks.

2. Observations and background star density

For a detailed description of our observing and reduction strategy, and additionally for the calibration procedure and the astrometric analysis using the proper motion diagram (PMD), we refer to Paper I. Table 1 contains the main properties of our four target stars and the related references, while in Table 2 we list our VLT/NACO observation log. Table 3 contains the astromet-

Send offprint requests to: Tobias Schmidt, e-mail: tobi@astro.uni-jena.de

\star Based on observations made with ESO telescopes at the Paranal Observatory under programme IDs 076.C-0292(A), 080.C-0424(A), 082.C-0489(A) and data obtained from the ESO/ST-ECF Science Archive Facility from the Paranal Observatory under programme ID 076.C-0579(A) and from the Hubble Space Telescope under programme ID SNAP-8216.

Table 1. Observed objects in Chamaeleon I

Object ^a	RA [h m s] ^{a,b}	Dec [$^{\circ}$ ' "] ^{a,b}	System architecture ^c	Bin. Ref.	Spectral types	SpT Ref.	Dist. [pc]	Dist. Ref.	2MASS K [mag] ^d	Backg. ^e density
DI Cha	11 07 20.72	-77 38 07.3	**+**	1,2,3	G2+M6+M5.5+M5.5	4,3	223 ^f	5	6.217	0.070
Sz 22	11 07 57.93	-77 38 44.9	**+w**	3,6,7	K7+M4.5+M2+M3	8,3,9	165	Cha I	6.830	0.070
CHXR 32	11 08 14.94	-77 33 52.2	*+**	10,3	G5+M1+M3.5	11,3	165	Cha I	6.182 ^g	0.070
Cha H α 5	11 08 24.11	-77 41 47.4	**	3	M6.5+M6.5	12,3	165	Cha I	10.711	0.091

Notes. ^(a) Taken from the SIMBAD database (Wenger et al. 2007). ^(b) International Celestial Reference System (ICRS) coordinates (epoch=J2000). ^(c) Updated multiplicity of the objects: *: star, **: binary, w**: wide binary stellar companion candidate, please see text for previously known multiplicity. ^(d) Skrutskie et al. (2006); Cutri et al. (2003). ^(e) expected number of background stars in the NACO S13 field of view (see text). ^(f) see text for a discussion. ^(g) value by Carpenter et al. (2002), as 2MASS only lists an upper limit, according to non-detection.

References. (1) Reipurth & Zinnecker (1993). (2) Simultaneously imaged by Lafrenière et al. (2008) and by us (here). (3) newly found (here). (4) Henize & Mendoza (1973). (5) van Leeuwen (2007). (6) Ghez et al. (1997). (7) Lafrenière et al. (2008). (8) Comerón et al. (1999). (9) Gómez & Mardones (2003). (10) Chelli et al. (1988). (11) Feigelson & Kriss (1989). (12) López Martí et al. (2004).

Table 3. Astrometric calibration results using the binary HIP 73357

JD - 2453700 [days]	Epoch	Pixel scale [mas/Pixel]	Orientation [$^{\circ}$]	Filter
88.84779	Feb 2006	13.24 \pm 0.18	0.18 \pm 1.24	Ks
815.91117	Feb 2008	13.22 \pm 0.20	0.73 \pm 1.40	J
815.91907	Feb 2008	13.25 \pm 0.20	0.68 \pm 1.40	Ks
1181.89936	Feb 2009	13.25 \pm 0.21	0.76 \pm 1.48	Ks

Notes. Hipparcos values (Perryman et al. 1997) were used as reference values. Measurement errors of Hipparcos as well as maximum possible orbital motion since the epoch of the Hipparcos observation, are taken into account.

ric calibration results and Table 4 the proper motion values used. The absolute and relative astrometric results are listed in Tables 5 and 6, respectively, while the resulting gradients of the variations in angular separations and in position angle are given in Tables 7 and 8, respectively, based on linear fits of the corresponding astrometric results. In Table 9 we summarize the differential photometry. In Figures 1 – 8 we present detailed maps and the proper motion diagrams (PMDs) for each of the stellar systems.

The last column of Table 1 refers to the expected number of fore- and background stars in the NACO S13 field (field of view 13.56 x 13.56 arcseconds), according to the star counts down to the 2MASS limiting magnitude (near K = 16 mag) in a cone of a radius of 300 arcseconds around each target. The mean density value of our four targets is 0.075 ± 0.009 , which is consistent with the average value 0.118 ± 0.030 of the 16 binaries and multiple systems in Cha, described in Paper I. Probably, the slightly lower background star number density by 1.4σ here occurs because these four stars are embedded in the central cloud of Cha I, with a stronger interstellar extinction A_V of 6.8 ± 1.9 mag according to an extinction map by Kainulainen et al. (2006) or 4.6 ± 0.8 mag according to an extinction map by Cambresy et al. (1997), while most targets in Paper I are distributed over a much larger area on the sky. This extinction value is in both cases a factor of 1.3 ± 0.4 higher than for all of the 16 multiple systems from Paper I within the region of the extinction maps, only weakly supporting the above-mentioned explanation, while a strong argument in favour of this hypothesis is that the objects SZ Cha, RX J1109.4-7627, and Sz 41 from Paper I, all being slightly outside the central region, possess only about 1.2 mag

Table 4. Proper motions

Object	Reference	$\mu_{\alpha} \cos \delta$ [mas/yr]	μ_{δ} [mas/yr]
DI Cha	Hipparcos (new) (1)	-24.61 \pm 1.84	3.45 \pm 1.54
	Tycho-2 (2)	-23.6 \pm 3.0	6.0 \pm 2.8
	used: UCAC 3 (3)	-15.8 \pm 1.6	-5.1 \pm 1.7
Sz 22	UCAC 3 (3)	-26.7 \pm 5.7	13.7 \pm 7.7
CHXR 32	UCAC 3 (3)	-2.1 \pm 5.6	-4.4 \pm 5.5
	PPMX (4)	-27.2 \pm 3.8	14.14 \pm 3.8
Cha H α 5	used: UCAC 2 (5)	-15.9 \pm 3.7	7.7 \pm 3.4
	PSSPMC (6)	-18 \pm 13	11 \pm 13
	SSS-FORS1 (7)	-31.8 \pm 21.7	12.5 \pm 21.7
	SSS-Sofi (7)	-29.6 \pm 11.8	9.7 \pm 11.8
	weighted mean	-25.4 \pm 8.1	10.6 \pm 8.1
Median Cha I	Luhman ^a (8)	-21 \pm \sim 1	2 \pm \sim 1

Notes. Only independent sources with individual error bars for the targets were considered. ^(a) Based on UCAC2 proper motions from (5)

References. (1) van Leeuwen (2007) (2) Høg et al. (2000) (3) Zacharias et al. (2010) (4) Röser et al. (2008) (5) Zacharias et al. (2004) (6) Ducourant et al. (2005) (7) own data (here) & Hambly et al. (2001) (8) Luhman et al. (2008)

extinction in contrast to the eight most central objects exhibiting on average about 4.3 mag of extinction (Cambresy et al. 1997).

3. Description of the individual stars

3.1. The quadruple system DI Cha

According to Guenther et al. (2007) and Melo (2003), DI Cha is spectroscopically a single star with a relatively high mass of $\sim 2.4 M_{\odot}$ and spectral type around G2 (Lommen et al. 2007). According to Tetzlaff et al. (2011), the star has an age of 2.7 ± 1.8 Myr and a mass of $2.0 \pm 0.1 M_{\odot}$. The Paschen β line appears in emission (Gómez & Mardones 2003), and Manoj et al. (2011) report that DI Cha is a Class II object with mid-IR excess emission arising from a protoplanetary disc surrounding it, but with relatively low mass ($\leq 0.009 M_{\odot}$, Lommen et al. 2007). Reipurth & Zinnecker (1993) detected a faint companion candidate at an angular separation $\sim 4.6''$, later resolved into a binary source itself by Lafrenière et al. (2008),

Table 2. VLT/NACO observation log

Object	Other name	JD - 2453700 [days]	Date of observation	DIT [s]	NDIT	Number of images	Airmass	DIMM ^b Seeing	τ_0^c [ms]	Filter
DI Cha	HIP 54365	83.85826	17 Feb 2006	0.3454	100	20	1.79	0.63	6.5	Ks
		815.62668	19 Feb 2008	0.3454	174	5	1.82	0.80	5.3	Ks
		815.63134	19 Feb 2008	1.2	50	5	1.81	0.84	4.7	J
		1182.64078 ^a	20 Feb 2009	0.3454	87	20	1.77	0.81	5.1	Ks
Sz 22	FK Cha	83.88427	17 Feb 2006	3	12	20	1.86	0.56	6.9	Ks
		815.64511	19 Feb 2008	4	15	5	1.77	0.86	4.7	Ks
		815.65010	19 Feb 2008	30	2	5	1.76	0.80	5.0	J
CHXR 32	Glass I / HP Cha	816.89621	20 Feb 2008	1/3	60/20	5/5	1.92	1.65	2.3	Ks
		1182.90637 ^a	20 Feb 2009	0.3454/0.5	87/120	12/6	1.97	0.52	8.9	Ks
Cha H α 5	ISO-ChaI 144	82.75127	16 Feb 2006	50	1	20	1.66	0.55	8.3	Ks
		816.68649	20 Feb 2008	60	1	5	1.70	0.79	4.8	Ks
		816.69139	20 Feb 2008	60	1	5	1.69	0.71	5.4	J
		1181.73805 ^a	19 Feb 2009	30	2	15	1.66	0.42	7.5	Ks

Notes. Each image consists of the number of exposures given in column 6 times the individual integration time given in column 5. ^(a) Data taken in cube mode, so each image is a cube of the number of planes given in column 6, each having the individual integration time given in column 5. ^(b) Differential image motion monitor (DIMM) seeing average of all images taken from the individual fits headers. ^(c) coherence time of atmospheric fluctuations.

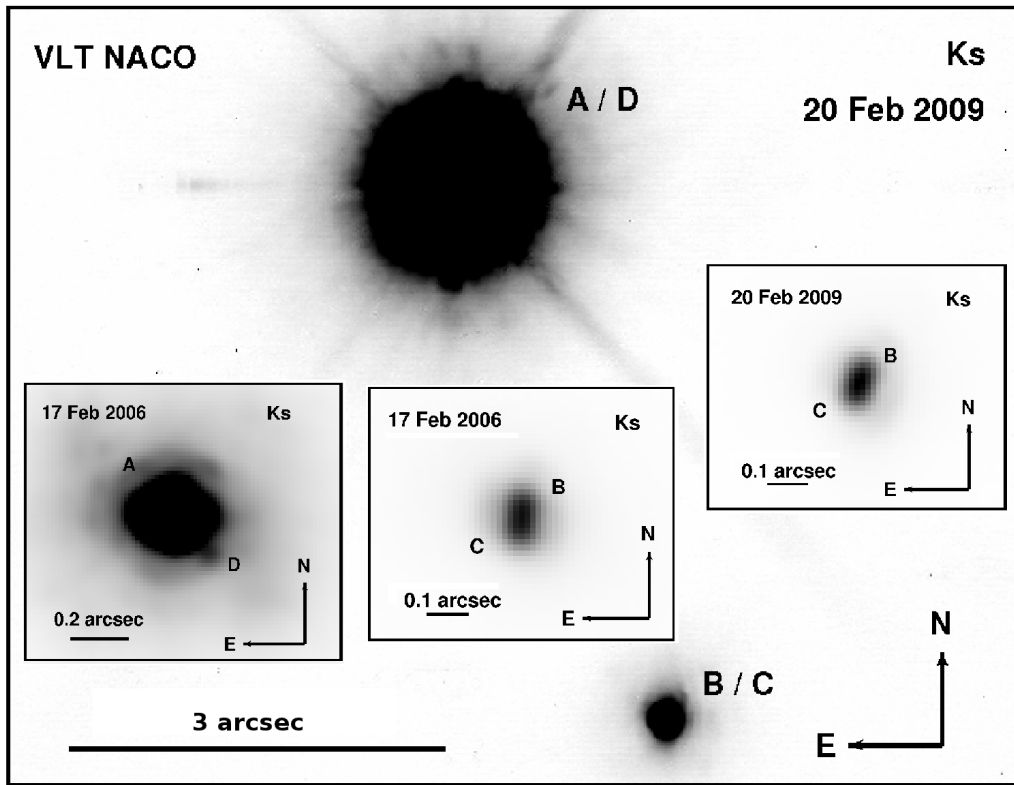


Fig. 1. VLT NACO Ks band images of DI Cha. Main frame: One of our observations of the first found binarity of DI Cha (Reipurth & Zinnecker 1993). *Inserts:* our new detected component D (left insert), and two images of the B/C pair at different epochs, revealing orbital motion in the position angle (central and right insert).

and separated by only $\sim 0.06''$ or 10 AU, denoted here as B and C. Here we present slightly earlier data of this triplicity from February 2006, as well as the first confirmation of the triple system, based on common proper motion, and not solely based on statistical arguments.

In addition to these three known components, our observations reveal another companion candidate at a separation of $0.2''$ from DI Cha A (Fig. 1), designated D. Our PMDs (Fig. 2) exclude the background hypothesis, and all four stars are co-

moving. However, there is no significant orbital motion of the fainter pair B/C around the primary pair A/D. On the other hand, both close pairs reveal significant orbital variations, especially of their position angles. That of pair B/C is compatible with an orbital period of about 65 years, that of A/D with about 130 years. It seems remarkable that this orbital motion seems to be clockwise in the case of B/C, but counter-clockwise in A/D. From the middle panels in Fig. 2 we find that because both the change in PA and separation are between the expectation for edge-on and

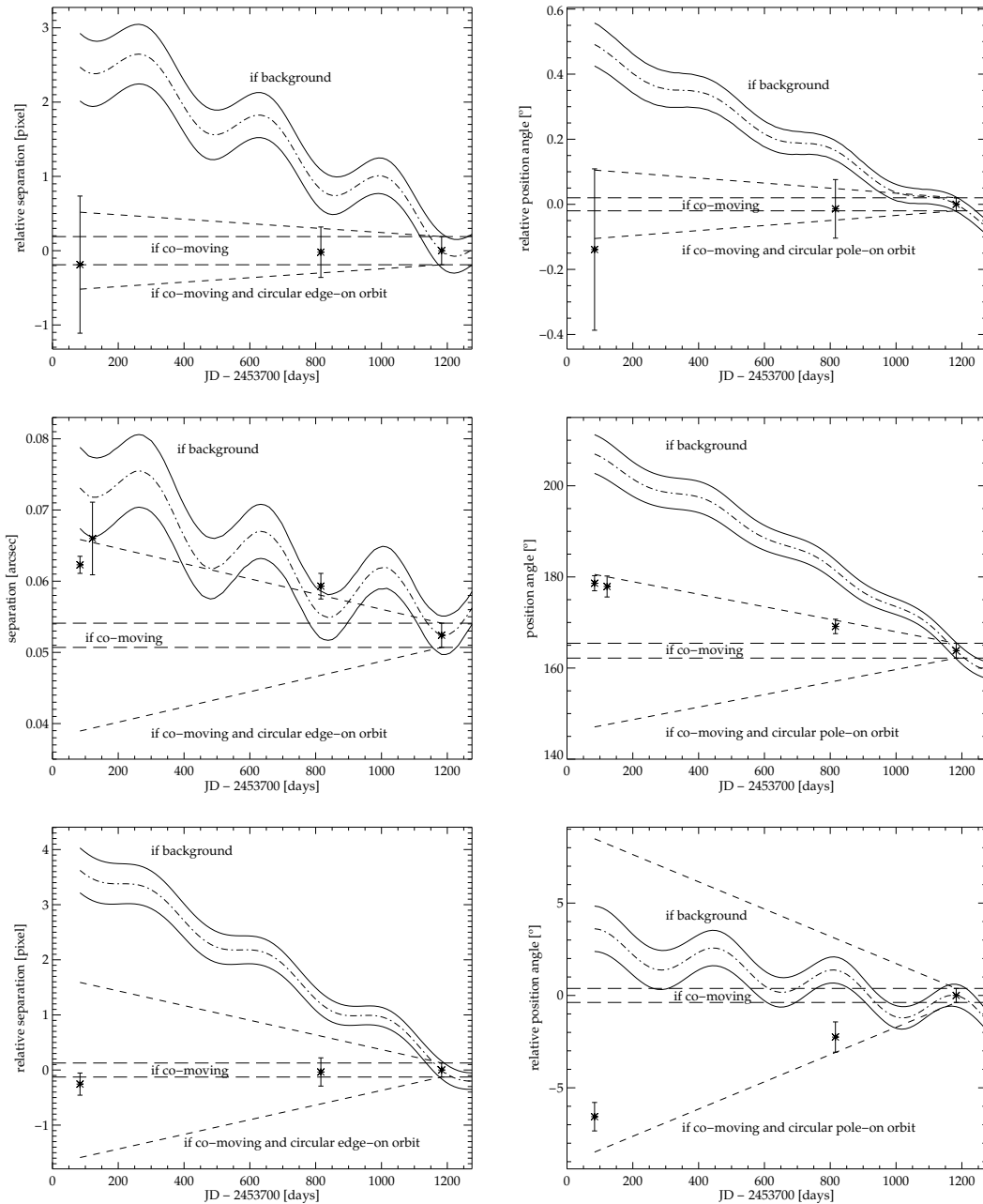


Fig. 2. Proper motion diagrams (PMD) of different components in the DI Cha quadruple system for separation (left) and position angle (right). *Top:* relative astrometric measurements of the centre of gravity of B/C (assuming being approx. the centre of light) relative to A. *Middle:* absolute astrometric measurements of the pair B/C. *Bottom:* relative astrometric measurements of D relative to A.

face-on orbits, we can conclude that the orbit inclination of DI Cha B & C lies between these two extremes or that the eccentricity is high. Likewise we find from the bottom panels that the (non-detection of a) change in separation, and that the change in PA is close to the expectation for a face-on orbit, we can conclude that the orbit of DI Cha D around the primary is face-on and/or that the eccentricity is high. These results mean that coplanarity of the orbits of DI Cha D around the primary and DI Cha C around B is impossible.

According to their magnitudes (Table 9), all three fainter components should be M type dwarfs. Although the magnitude of DI Cha D is similar to that of Cha H α 2 B, which is a brown dwarf candidate (Schmidt et al. 2008b), the larger parallactic

distance to the DI Cha system of 223 ± 79 pc (van Leeuwen 2007) diminishes the probability of a brown dwarf classification of DI Cha D. In Bertout et al. (1999) the authors confirm that YSOs are located in their associated clouds, as anticipated by a large body of work, and discuss reasons that make the individual parallaxes of some YSOs doubtful. They discuss that Chamaeleon I is at the previously anticipated distance and finally find DI Cha to be at 194 ± 58 pc if single. We therefore assume that DI Cha is at the distance of Cha I, with a best distance estimate of 165 ± 30 pc as discussed in Schmidt et al. (2008a).

On the basis of these previous assumptions we used the COND evolutionary models (Baraffe et al. 2003), the BCAH models (Baraffe et al. 1998, 2002), and the temperature (to spec-

tral type conversion) scale of Luhman et al. (2003) to estimate a spectral type of $M6 \pm 1.5$ for the new companion. While the same models give a best mass estimate above the lower stellar limit, the lower 1σ mass errors point to a minimum mass of $\geq 67 M_{\text{Jup}}$ for DI Cha D, justifying a brown dwarf candidate classification.

The same procedure results in a spectral type of $M5.5 \pm 1.5$ for the components B and C, just above the brown dwarf – stellar mass boundary and much later than the spectral type K0 found by Kraus & Hillenbrand (2007). Common for all three low-mass companions DI Cha B – D is that their J-Ks colour is too red for their estimated spectral types (Table 9).

While we could already prove that DI Cha D is 82 % likely to be a real companion candidate, inspecting the speckle pattern of our individual measurements in the first epoch with a new code¹ developed in R by Haase (2009), we can confirm this result by using all three epochs of DI Cha D, showing a linear counter-clockwise orbital motion (Fig. 2, Tables 7 & 8).

3.2. The binary Sz 22

This target has hitherto been considered (spectroscopically) as a single star (Melo 2003; Haisch et al. 2004), but it has a known companion candidate at an angular separation of ~ 17.6 arcsec (Ghez et al. 1997), outside of our field of view (FoV). Taking its strong interstellar extinction of $A_v \sim 7$ mag into account, its spectral type corresponds to K6 (Furlan et al. 2009; Luhman 2007). This extinction and the Paschen β emission (Gómez & Mardones 2003) could indicate the presence of a circumstellar disc, which is directly visible on images taken from the archive of the Hubble Space Telescope, as well as from our VLT NACO Ks band images (Fig. 3). This feature was described for the first time as a nebulous object with dimensions of $4'' \times 7''$ with the longer dimension at a position angle of 160° in Henize & Mendoza (1973). In the optical HST image, we find dimensions of $3'' \times 5''$ with the longer dimension at a position angle of $\sim 155^\circ$, while there seems to be a slight change in orientation in the near-IR using NACO, where we find dimensions of $2.5'' \times 5''$ with the longer dimension at a position angle of $\sim 145^\circ$. The dimensions seem to shrink with time, while the orientation changes clockwise. However, Lommen et al. (2007) find out that the disc has a relatively low mass ($\leq 0.009 M_\odot$).

Nevertheless, this object could also be an embedded YSO surrounded by a compact reflection nebula having a large infrared excess, which shows a compact north-south flow HH 920 emerging from it (Bally et al. 2006), consistent with its strong interstellar extinction of $A_v \sim 7$ mag despite its flat appearance, as well as the estimated age of the star of ≤ 0.1 Myr (Gómez & Mardones 2003). However, we find a best fitting age of about 1.4 Myr, based on BCAH evolutionary models (Baraffe et al. 1998, 2002). For this purpose, the strong interstellar extinction of $A_v \sim 7$ mag was transformed to K band according to the interstellar extinction law values by Rieke & Lebofsky (1985), and the spectral type K6 (Furlan et al. 2009; Luhman 2007) was converted to temperature based on stellar colours of Table A5 in Kenyon & Hartmann (1995). In any case, Sz 22 is slightly below the average age of Cha I members, which is close to 2 Myr (Comerón et al. 2000), or even one of the youngest members in this star-forming region.

The new stellar companion is located ~ 0.5 arcsec west of the primary star, just outside the detected disc/reflection nebula (Fig. 3). Our PMDs (Fig. 4) confirm that both components are co-

moving and that the companion increases its angular separation from the primary by 2.5 mas each year, without changing its position angle. Because the change in separation is close to the expectation for an edge-on orbit, we can conclude that the orbit is almost edge-on, or else that the eccentricity is high. As the extended emission around the primary could either be a disc or a compact reflection nebula, we cannot judge whether the disc around Sz 22 A and the probable edge-on orbit of Sz 22 A & B are aligned.

The disc/reflection nebula and its strong extinction make it difficult to classify the spectral type of the stellar companion; its J-Ks colours indicate an early M type, and its Ks band brightness is consistent with a spectral type of $M4.5 \pm 1.5$ using the procedure described for the companion of DI Cha, if the companion of Sz 22 is not extincted.

The wide visual companion candidate at ~ 17.6 arcsec (Ghez et al. 1997) cannot be astrometrically proven by us, since it is outside of our FoV, but it was shown to be binary by Lafrenière et al. (2008). According to the brightness ratio given there, we find spectral types of $M2 \pm 2$ and $M3 \pm 2$ using the method described in the previous section.

3.3. The triple system CHXR 32

According to Melo (2003) and Nguyen et al. (2012), CHXR 32 is spectroscopically single. However, this star, also named Glass I, is a well known binary of about 2.4 arcsec separation (Chelli et al. 1988). We here follow the notation of Correia et al. (2006), naming as “A” the eastern component, although it is fainter than “B” at optical wavelengths owing to a strong circumstellar extinction. CHXR 32 A is a G-type emission line star ($H\alpha$ emission equivalent width $< 10 \text{ \AA}$, hence a WTTS), possibly surrounded by a disc that diminishes the optical flux. For component B a spectral type K4 was determined (Reipurth & Zinnecker 1993, there denominated as “A”).

When we again reduced the data used by us as our first epoch (but originally from Lafrenière et al. 2008), we noticed that the object B had an elongated shape. Using IDL Starfinder (Diolaiti et al. 2000), we fitted the point-spread-function (PSF) of A to this component, revealing the best fit for a double source at this position. To confirm this and to search for common proper motion, we obtained a new NACO image in 2009 that clearly separates the two components of B, with only 0.08 arcsec angular separation, now called B and C (Fig. 5). The corresponding PMDs (Fig. 6) confirm that all three components are co-moving. There are no significant orbital movements in the wide pair A-BC; however, there are strong indications of orbital variations in position angle and especially in the separation between B and C, which increases at a rate of nearly 10 mas/year, facilitating the direct detection of this binary in 2009 (Tables 7 & 8). From the strong change in separation close to the expectation for an edge-on orbit, we can conclude that the orbit is close to edge-on, or that the eccentricity is high. Although the PMD of the separation variation between B and C is compatible with the background hypothesis, the variations in the position angle are not compatible with those of a background star.

As for the other targets, we used the brightnesses of the primaries to determine mean apparent magnitudes of the secondaries using the measured contrasts and assuming no significant variations; however, as for CHXR 32 A, 2MASS only gives upper limits in the H and K bands, so we use the brightnesses of $H = 7.189 \pm 0.114$ mag and $Ks = 6.182 \pm 0.089$ mag given in Carpenter et al. (2002), reflecting the strong extinction of the

¹ available at <http://www.cran.r-project.org/web/packages/ringscale/>

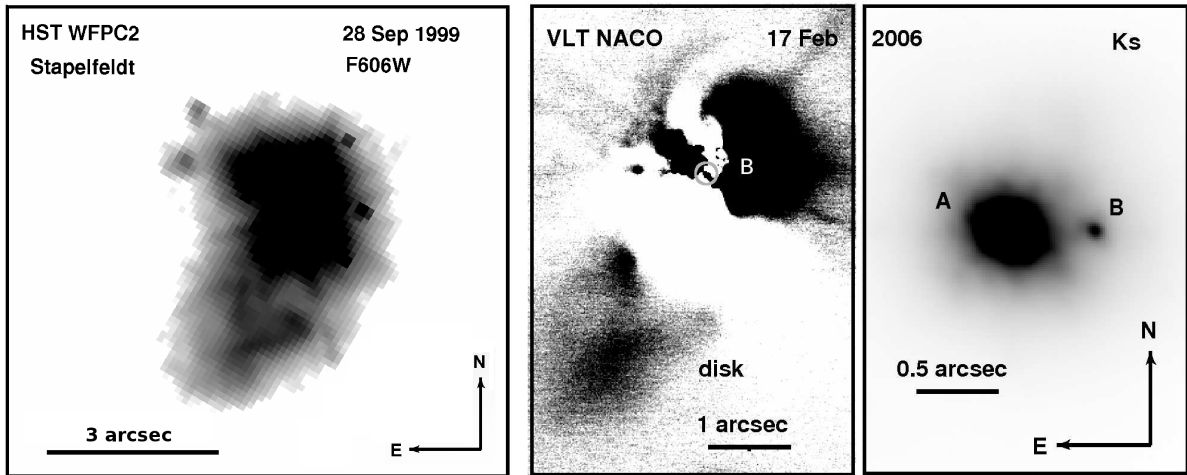


Fig. 3. Sz 22 and its surroundings: Images of the circumstellar disc/reflection nebula in the visual band pass (HST, left) and in the infrared (VLT NACO Ks band, centre). The right frame shows Sz 22 with its newly detected stellar companion B (same image as in the centre, but without PSF subtraction of the primary positioned at the light grey circle in the central image). Please see text for further information.

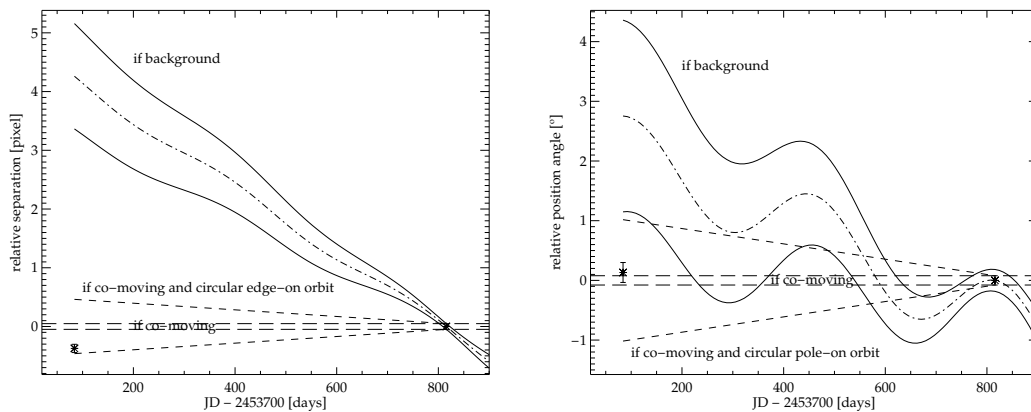


Fig. 4. PMDs of Sz 22 from the relative astrometric measurements for separation (left) and position angle (right).

primary. According to the photometry (Table 9) the secondary component of this now resolved triple star consists of an M1 (K6–M3.5) type star with an M3.5 (M2.5–M5.5) companion, compatible with the unresolved H-Ks colour measured for B & C. We note, however, that there are strong systematic errors because the J band brightness varies by 2.3σ between 2MASS and Carpenter et al. (2002), while the visible light curve varies up to about 2 mag according to ASAS data presented in Kruger et al. (2013).

Since the B & C components could not be fitted individually using PSF fitting in the J band data from 2006 and Ks band data from 2008 (Table 9), we used the dedicated aperture photometry routines from ESO-MIDAS (Banse et al. 1992) to measure a combined brightness difference relative to component A, because PSF fitting using the single PSF of CHXR 32 A as comparison leads to overestimated brightness differences owing to a slight elongation of the combined light of B & C.

For the creation of the PMDs mentioned above, we decided to use the proper motion of UCAC2 (Zacharias et al. 2004) instead of UCAC3 (Zacharias et al. 2010), since this proper motion value is consistent with the proper motion of Cha I. The present discrepancy in UCAC3 can most likely be explained by the inclusion of 140 catalogues of all kinds in different wave-

length bands. If epochs from near-infrared catalogues, in which the extincted CHXR 32 A is dominant, are mixed with those from optical catalogues, in which CHXR 32 BC are the dominant sources, the spatial separation of ~ 2.4 arcsec between A & BC can be misinterpreted as a deviation from the real proper motion within the epoch differences of several years. The strong photometric variability in ASAS data between 2002 to 2004 in CHXR 32 A reported in Kruger et al. (2013), could lead to further discrepancies. Please see this publication for further discussion of the proper motion behaviour of the system.

3.4. The unresolved binary Cha H α 5

This target attracted early attention after Neuhäuser et al. (2002) found a candidate for a sub-stellar companion just $1.5''$ away from Cha H α 5. Based on its low apparent luminosity, this object could even have been of planetary mass. However, applying optical (FORIS1) and infrared (ISAAC) spectroscopy, Neuhäuser et al. (2003) show that it is a background object. Here, we confirm this conclusion for the first time based on astrometric observations at three epochs (Figs. 7 & 8).

During this investigation we noticed that Cha H α 5 had elongated images (Fig. 7), while the PSF of the background object

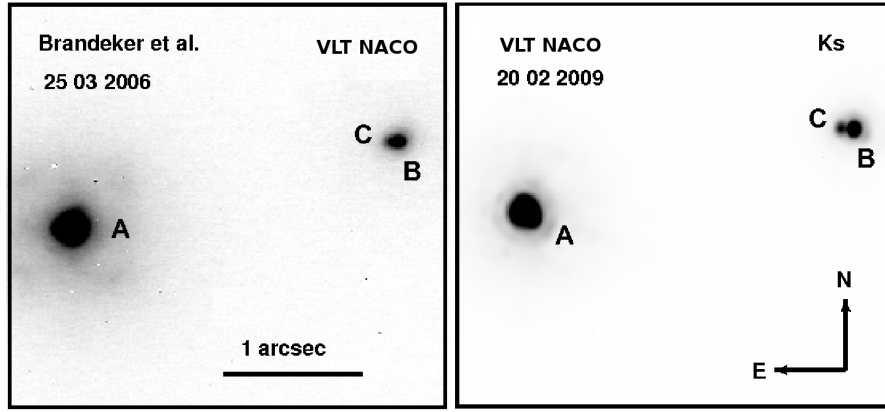


Fig. 5. VLT NACO Ks band images of CHXR 32. The left frame shows the first observation by Brandeker et al. (Lafrenière et al. 2008) as reduced again by us with an elongated PSF of the component B/C. The right frame, taken by us nearly three years later as a second epoch, confirms the triple nature of this target, showing two resolved PSFs of B and C.

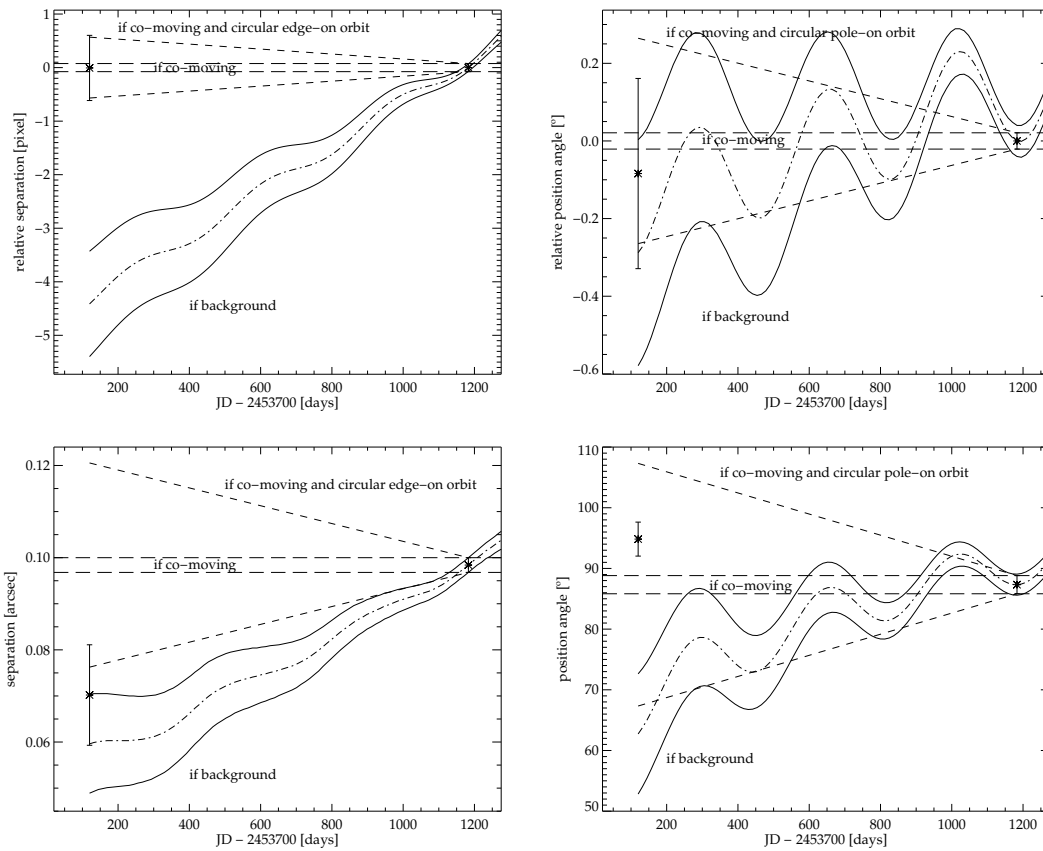


Fig. 6. PMDs of CHXR 32 from the relative and absolute astrometric measurements for separation (left) and position angle (right). The upper panels refer to the centre of mass of the pair B/C (adopting that the mass of B is 1.5 times that of C), relative to the main component A. The separation PMD rejects here the background hypothesis. The lower panels are PMDs of C relative to B, assuming that the proper motion of B is identical to that of A. Here the background hypothesis is excluded by the position angle PMD.

appeared perfectly circular. This should not be the case if the elongation was caused by problems with the adaptive optics, especially because Cha H α 5 was used as AO guide star. Therefore, we fitted the PSF of the background object to the images of Cha H α 5, obtained in 2006 and 2009 (those of 2008 had too bad a quality owing to adverse weather conditions), using the IDL Starfinder software (Diolaiti et al. 2000). In both cases the best

fit revealed two components of only ~ 0.05 arcsec separation, just below the theoretical resolution limit of NACO/UT4 of 68 mas.

The PMDs (Fig. 8) show that this close pair is co-moving. There is no significant change in the angular separation between 2006 and 2009, but a strong variation in the position angle, corresponding to an orbital period of about 46 years. This is consistent with two stellar components of $0.12 M_{\odot}$ each, according to Kepler's third law. The projected separation between both com-

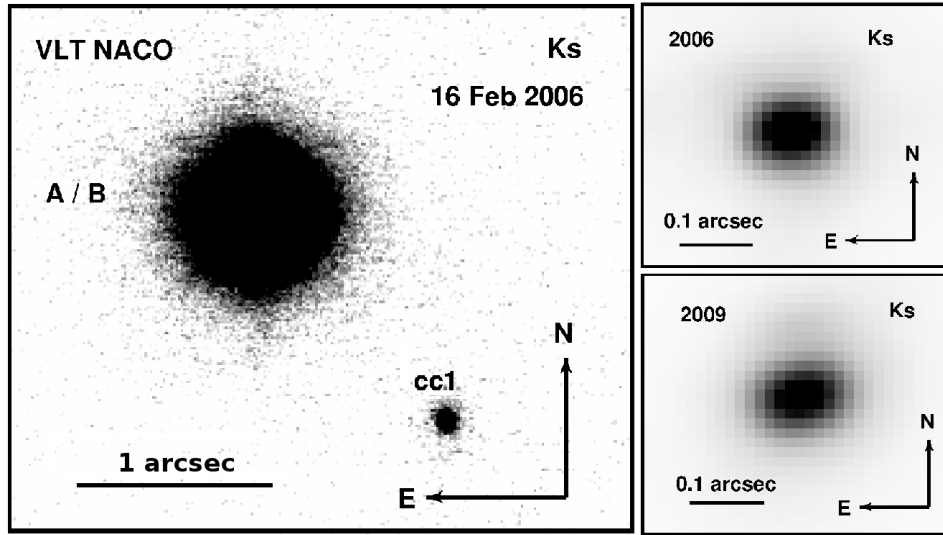


Fig. 7. VLT NACO Ks band images of Cha H α 5. *Left:* Our first observation in 2006 revealed a slightly elongated PSF of the primary (designated A/B), compared to the PSF of the much fainter background object cc1. *Right:* the position angle (orientation) of the elongation caused by the presence of two components has changed from the epochs in 2006 to 2009, confirming orbital motion of this (still unresolved) binary.

ponents is about 8 AU (adopting 165 pc distance from the Sun), just outside the range in which Joergens (2008) could find companions with the radial velocity method, in this way linking both methods and thus avoiding any blind gap of detection possibility. The short period, visible only in the position angle (circular pole-on orbit), will soon enable confirmation of a curved orbital motion.

The resolved brightnesses of Cha H α 5 A & B are compatible with spectral types of M6.5 (M5–M7) for both components, using the BCAH and COND evolutionary models, and are thus fully consistent with M6 (Neuhäuser & Comeron 1998) and M6.5 (López Martí et al. 2004) for an assumed age of 2 Myr, which most of the members of Cha I are (Comerón et al. 2000), but in contrast to earlier estimates of 0.4 Myr (Gómez & Mardones 2003). There seems to be some resemblance to the Cha H α 2 system (Schmidt et al. 2008b), but with a much shorter orbital period. The distances from the Sun of both systems are comparable, while the magnitudes are only slightly fainter, therefore we cannot exclude that Cha H α 5 B and even A are brown dwarfs. The corresponding 1σ error minimum masses of the components are 68 & 65 M_{Jup} according to COND models, respectively.

As given in the previous section for part of the photometry of CHXR 32 A(BC), we can only measure a brightness difference of cc1 with respect to the combined light of components A & B in the data of 2008, using aperture photometry with ESO-MIDAS.

4. Conclusions

The search for stellar and sub-stellar companions of young low-mass stars is one of our main aims, where we apply high-precision astrometry in the JHKs band passes at different epochs over several years. With the VLT NACO instrument we can, this way, resolve binary separations of $0.07''$, corresponding to projected linear separations of 6 – 10 AU between the closest components (depending on the adopted distance to the Cha star-forming regions). But even below this limit, we found the unre-

Table 7. Projected orbital separations and linear orbital movement fit results from absolute astrometric measurements

Object	proj. sep. [AU]	Change in separation [mas/yr]	Change in PA ^a [°/yr]
DI Cha A(BC) ^b	755	-3.70 ± 5.45	0.04 ± 0.10
BC	10	-2.99 ± 0.65	-4.86 ± 0.68
AD	35	1.16 ± 1.76	2.18 ± 0.68
Sz 22 AB	85	2.50 ± 5.17	-0.07 ± 0.93
CHXR 32 A(BC) ^b	401	-0.91 ± 4.43	0.01 ± 0.18
A(BC) ^c	398	0.03 ± 17.4	0.03 ± 0.67
BC	14	9.69 ± 3.79	-2.58 ± 1.09
Cha H α 5 AB	8	-0.76 ± 1.20	7.84 ± 3.04
(AB)cc1 ^d	(232)	-9.90 ± 9.51	-0.38 ± 0.62

Notes. ^(a) PA is measured from N over E to S. ^(b) See ^d in Table 5. ^(c) See ^e in Table 5. ^(d) See ^f in Table 5.

Table 8. Projected orbital separations and linear orbital movement fit results from relative astrometric measurements

Object	proj. sep. [AU]	Change in separation [mas/yr] ^a	Change in PA ^b [°/yr]
DI Cha A(BC) ^c	755	0.61 ± 3.37	0.03 ± 0.06
BC	10	-2.89 ± 0.54	-4.94 ± 0.44
AD	35	1.12 ± 1.05	2.18 ± 0.28
Sz 22 AB	85	2.47 ± 0.56	-0.07 ± 0.09
CHXR 32 A(BC) ^c	401	0.30 ± 2.23	-0.01 ± 0.07
A(BC) ^d	398	0.03 ± 2.79	0.03 ± 0.08
BC	14	9.69 ± 3.73	-2.58 ± 0.87
Cha H α 5 AB	8	-0.75 ± 1.14	7.84 ± 2.97
(AB)cc1 ^e	(232)	-10.6 ± 1.99	-0.41 ± 0.10

Notes. ^(a) Using a nominal pixel scale of 0.01324 arcsec/pixel to convert from pixel to mas ^(b) PA is measured from N over E to S. ^(c) See ^d in Table 5. ^(d) See ^e in Table 5. ^(e) See ^f in Table 5.

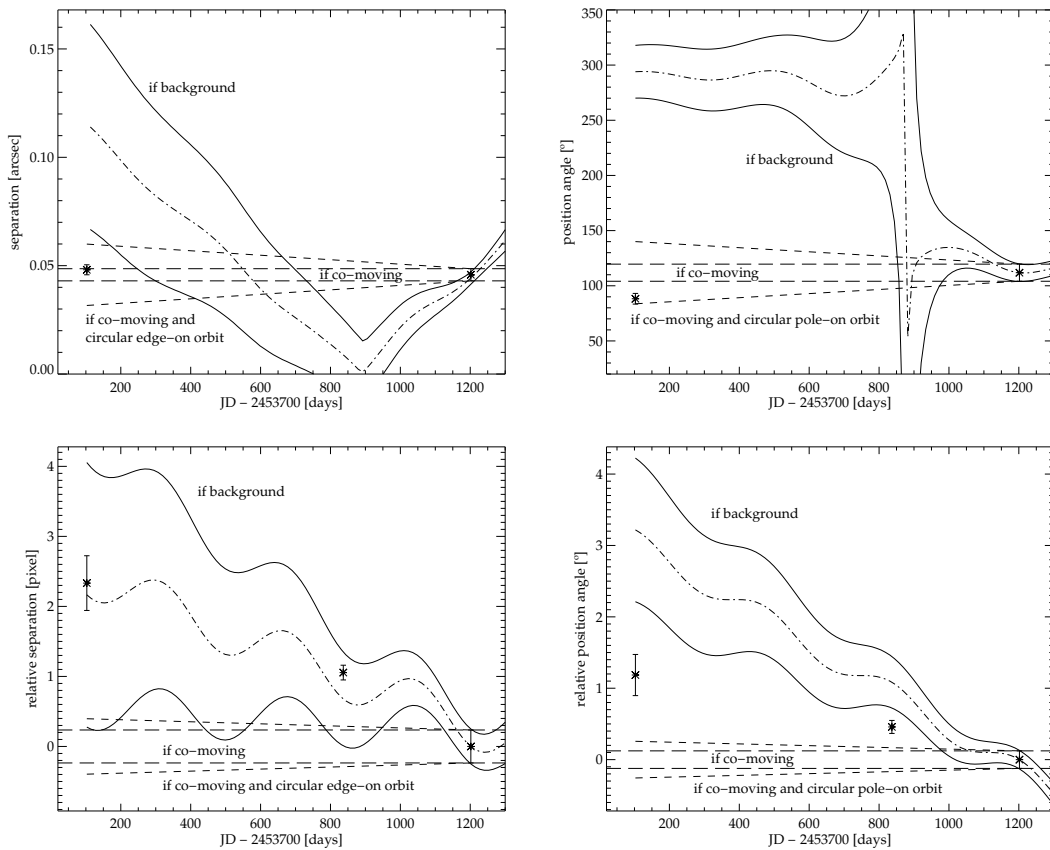


Fig. 8. PMDs of Cha H α 5 from the absolute and relative astrometric measurements for separation (left) and position angle (right). The upper panels refer to the co-moving A/B pair, the lower ones to the background object cc1 relative to A.

solved binary Cha H α 5 at a separation of less than 0.05'' due to its elongated PSF, which could be analysed using the PSF fitting method with dedicated software. This limit connects our astrometric method of multiplicity detection to that of the orbit determination via radial velocity measurements, filling in the still present lack of detecting projected binary separations in the range 3 – 10 AU in very young nearby star-forming regions at intermediate distances of about 150 pc (Joergens 2008) or as the Chamaeleon I complex at 165 ± 30 pc (see Schmidt et al. (2008a) for a discussion).

The VLT observations have a wide range of coverage in brightness, down to $K_s \sim 20$ mag, enabling the detection of sub-stellar companions as brown dwarfs and planets. In the Cha regions, however, such objects seem to be rather scarce. Only one radial velocity example named Cha H α 8 (Joergens & Müller 2007) and two examples from imaging, CHXR 73 (Luhman et al. 2006) and CT Cha (Schmidt et al. 2008a), as well as two other candidates have been identified so far, Cha H α 2 (Schmidt et al. 2008b) and T Cha (Huélamo et al. 2011), the latter additionally using the sparse aperture masking technique. Other rejected candidates found by us, as well as the corresponding sub-stellar statistics, will be presented in a forthcoming paper. In contrast, stellar companions are very frequent, and in Paper I we were able to confirm the physical reality of thirteen binaries and three triple systems. The present paper presents four additional cases, two binaries, one triple, and one quadruple system. In each of these four targets we were able to detect a hitherto unknown companion and confirm that these objects are co-moving and showing some kind of orbital motion with high probability.

While all four newly found stellar companions in this publication are part of the Cha I star-forming region², each object is individually of special interest. DI Cha is to our best knowledge the first directly resolved quadruple star system in Chamaeleon, for which in addition orbital motion of both hierarchical pairs could be derived and is presented in Tables 7 & 8. Around the star Sz 22 we could identify a stellar co-moving companion, as well as a prominent disc/reflection nebula of ≥ 2.5 arcsec size, corresponding to ≥ 410 AU. Since a temperature of about 1300 K, needed to be visible thermally in the Ks band, is very unlikely despite its youth, the disc/nebula must be seen in reflection. Since the primary, as a K7 star, might be too faint in the optical for such a strong reflective luminosity of the disc/nebula, we assume that the disc/nebula is illuminated by HD 97048, an A0 star at ~ 37 arcsec projected separation, corresponding to ~ 5900 AU at the distance of HD 97048 of 158 ± 16 pc (van Leeuwen 2007), which is itself surrounded by a large directly detected disc of ~ 700 AU (Doering et al. 2007) found using the Hubble Space Telescope.

CHXR 32, often also called Glass I, was known to be a star with infrared companion. While the nature of the infrared companion can be explained by a G-star weakened in the optical by an edge-on disc, Kruger et al. (2013) find difficulties fitting the spectrum of CHXR 32 B (called Glass Ia there). They can fit an X-Shooter spectrum by including a mid K-type stellar source, as

² In the inner 7×14 arcmin part of the Cha I complex centred on HD 97048, as presented e.g. in an official poster of ESO created using data from the instrument FORS at <http://www.eso.org/public/images/eso9921c/>

well as an early M dwarf, which is needed to fit the CO overtone absorption feature at 2300 nm. This is fully consistent with our resolved triple nature of CHXR 32, although at the edge of our allowed spectral classification and in good agreement with the apparent magnitudes in Table 9. A spectral type of K4, as given by Chelli et al. (1988), is slightly outside the spectral class range we found for CHXR 32 B, but might be influenced by the previously unknown multiplicity. A classification as K6 in Luhman (2004a) is just within the spectral range determined by us. Finally, Cha H α 5 is the closest stellar companion found in this survey, but is not even fully resolved. The components are still brown dwarf candidates as discussed for the fainter component of the very similar case of Cha H α 2 (Schmidt et al. 2008b), while this new binary has a much lower separation, hence an orbital period of about 46 years, which will very soon allow curvature to be detected in the orbital motion.

We cannot exclude DI Cha D and Cha H α 5 A and B being brown dwarfs, because their 1σ error minimum masses, which are 67, 68 and 65 M_{Jup} using their brightnesses (Table 9) and COND evolutionary models (Baraffe et al. 2003) at 1 Myr age and minimum distance, respectively, are below the mass of the least massive stars of 75 M_{Jup} (Basri 2000). However, at the nominal distance of Cha I of 165 pc all sub-stellar candidate objects have masses $\geq 78 M_{\text{Jup}}$ even if we assume very young ages of 1 Myr. Both components of Cha H α 5 have masses of about 0.12 M_{\odot} each ($\geq 83 M_{\text{Jup}}$ at 1σ error) as calculated using Kepler's third law and assuming a strictly pole-on orbit and the measured orbital motion of the Cha H α 5 system within our two epochs (Tables 7 & 8). Comparable masses of about 0.11 and 0.124 M_{\odot} were found for the similar binary system Cha H α 2 on the basis of photometric and spectroscopic observations (Schmidt et al. 2008b). If the total mass of the system was found to be $\leq 0.2 M_{\odot}$, Cha H α 5 would be a new member for the Very Low Mass Binaries Archive (Siegler 2007), currently being composed from 99 systems, e. g. 2MASS J11011926-7732383 AB (Luhman 2004b) and Cha H α 8 AB (Joergens & Müller 2007) as members of Cha I. DI Cha D, on the other hand, possesses a brightness difference (Table 9) comparable to the recently found brown dwarf companion PZ Tel B (Mugrauer et al. 2010; Biller et al. 2010) at even smaller angular separation to its primary, while most likely having a stellar nature due to its primary's higher mass.

Acknowledgements. We would like to thank the ESO Paranal Team, the ESO User Support department, and all the other very helpful ESO services as well as the anonymous referee, the 2 editors, C. Bertout and T. Forveille, and the language editor J. Adams, for helpful comments. Moreover, we thank D. Haase for providing his speckle pattern detection program 'ringscale'.

TOBS acknowledges support from the Evangelisches Studienwerk e.V. Villigst. NV acknowledges support by the Comité Mixto ESO-Gobierno de Chile, as well as by the Gemini-CONICYT fund 32090027. TOBS, RN & TR would like to acknowledge support from the German National Science Foundation (Deutsche Forschungsgemeinschaft, DFG) in grant NE 515/30-1, AB & RN would like to acknowledge financial support from projects NE 515/13-1 and NE 515/13-2, and TR & RN would further like to acknowledge financial support under the project numbers NE 515/23-1 and NE 515/36-1.

HST data were obtained from the data archive at the Space Telescope Institute, which is operated by the association of Universities for Research in Astronomy, Inc. under NASA contract NAS 5-26555. This publication makes use of data products from the Two Micron All Sky Survey, which is a joint project of the University of Massachusetts and the Infrared Processing and Analysis Center/California Institute of Technology, funded by the National Aeronautics and Space Administration and the National Science Foundation. This research made use of the VizieR catalogue access tool and the Simbad database, both operated at the Observatoire de Strasbourg. This research makes use of the Hipparcos Catalogue, the primary result of the Hipparcos space astrometry mission, undertaken by the European Space Agency. This research made use of NASA's Astrophysics Data System Bibliographic Services. This publication made use of the Very-Low-Mass Binaries Archive housed at

<http://www.vlmbinaries.org> and maintained by Nick Siegler, Chris Gelino, and Adam Burgasser.

References

- Bally, J., Walawender, J., Luhman, K. L., & Fazio, G. 2006, *AJ*, 132, 1923
 Banse, K., Grosbol, P., & Baade, D. 1992, in *Astronomical Society of the Pacific Conference Series*, Vol. 25, *Astronomical Data Analysis Software and Systems I*, ed. D. M. Worrall, C. Biemesderfer, & J. Barnes, 120
 Baraffe, I., Chabrier, G., Allard, F., & Hauschildt, P. H. 1998, *A&A*, 337, 403
 Baraffe, I., Chabrier, G., Allard, F., & Hauschildt, P. H. 2002, *A&A*, 382, 563
 Baraffe, I., Chabrier, G., Barman, T. S., Allard, F., & Hauschildt, P. H. 2003, *A&A*, 402, 701
 Basri, G. 2000, *ARA&A*, 38, 485
 Bertout, C., Robichon, N., & Arenou, F. 1999, *A&A*, 352, 574
 Biller, B. A., Liu, M. C., Wahhaj, Z., et al. 2010, *ApJ*, 720, L82
 Cambresy, L., Epchtein, N., Copet, E., et al. 1997, *A&A*, 324, L5
 Carpenter, J. M., Hillenbrand, L. A., Skrutskie, M. F., & Meyer, M. R. 2002, *AJ*, 124, 1001
 Chelli, A., Cruz-Gonzalez, I., Zinnecker, H., Carrasco, L., & Perrier, C. 1988, *A&A*, 207, 46
 Comerón, F., Neuhäuser, R., & Kaas, A. A. 2000, *A&A*, 359, 269
 Comerón, F., Rieke, G. H., & Neuhäuser, R. 1999, *A&A*, 343, 477
 Correia, S., Zinnecker, H., Ratzka, T., & Sterzik, M. F. 2006, *A&A*, 459, 909
 Cutri, R. M., Skrutskie, M. F., van Dyk, S., et al. 2003, *2MASS All Sky Catalog of point sources.*, ed. R. M. Cutri, M. F. Skrutskie, S. van Dyk, C. A. Beichman, J. M. Carpenter, T. Chester, L. Cambresy, T. Evans, J. Fowler, J. Gizis, E. Howard, J. Huchra, T. Jarrett, E. L. Kopan, J. D. Kirkpatrick, R. M. Light, K. A. Marsh, H. McCallon, S. Schneider, R. Stiening, M. Sykes, M. Weinberg, W. A. Wheaton, S. Wheelock, & N. Zacarias
 Diolaiti, E., Bendinelli, O., Bonaccini, D., et al. 2000, in *Presented at the Society of Photo-Optical Instrumentation Engineers (SPIE) Conference*, Vol. 4007, *Proc. SPIE Vol. 4007*, p. 879-888, *Adaptive Optical Systems Technology*, Peter L. Wizinowich; Ed., ed. P. L. Wizinowich, 879-888
 Doering, R. L., Meixner, M., Holfeltz, S. T., et al. 2007, *AJ*, 133, 2122
 Ducourant, C., Teixeira, R., Périé, J. P., et al. 2005, *A&A*, 438, 769
 Feigelson, E. D. & Kriss, G. A. 1989, *ApJ*, 338, 262
 Furlan, E., Watson, D. M., McClure, M. K., et al. 2009, *ApJ*, 703, 1964
 Ghez, A. M., McCarthy, D. W., Patience, J. L., & Beck, T. L. 1997, *ApJ*, 481, 378
 Gómez, M. & Mardones, D. 2003, *AJ*, 125, 2134
 Guenther, E. W., Esposito, M., Mundt, R., et al. 2007, *A&A*, 467, 1147
 Haase, D. 2009, Report about Student Research Project, Univ. Jena
 Haisch, Jr., K. E., Greene, T. P., Barsony, M., & Stahler, S. W. 2004, *AJ*, 127, 1747
 Hambly, N. C., MacGillivray, H. T., Read, M. A., et al. 2001, *MNRAS*, 326, 1279
 Henize, K. G. & Mendoza, E. E. 1973, *ApJ*, 180, 115
 Høg, E., Fabricius, C., Makarov, V. V., et al. 2000, *A&A*, 355, L27
 Huéramo, N., Lacour, S., Tuthill, P., et al. 2011, *A&A*, 528, L7
 Joergens, V. 2008, *A&A*, 492, 545
 Joergens, V. & Müller, A. 2007, *ApJ*, 666, L113
 Kainulainen, J., Lehtinen, K., & Harju, J. 2006, *A&A*, 447, 597
 Kenyon, S. J. & Hartmann, L. 1995, *ApJS*, 101, 117
 Kraus, A. L. & Hillenbrand, L. A. 2007, *ApJ*, 662, 413
 Kruger, A. J., Richter, M. J., Carr, J. S., et al. 2013, *ApJ*, 764, 127
 Lafrenière, D., Jayawardhana, R., Brandeker, A., Ahmic, M., & van Kerkwijk, M. H. 2008, *ApJ*, 683, 844
 Lenzen, R., Hartung, M., Brandner, W., et al. 2003, in *Presented at the Society of Photo-Optical Instrumentation Engineers (SPIE) Conference*, Vol. 4841, *Instrument Design and Performance for Optical/Infrared Ground-based Telescopes*. Edited by Iye, Masanori; Moorwood, Alan F. M. *Proceedings of the SPIE*, Volume 4841, pp. 944-952 (2003)., ed. M. Iye & A. F. M. Moorwood, 944-952
 Lommen, D., Wright, C. M., Maddison, S. T., et al. 2007, *A&A*, 462, 211
 López Martí, B., Eisloffel, J., Scholz, A., & Mundt, R. 2004, *A&A*, 416, 555
 Luhman, K. L. 2004a, *ApJ*, 602, 816
 Luhman, K. L. 2004b, *ApJ*, 614, 398
 Luhman, K. L. 2007, *ApJS*, 173, 104
 Luhman, K. L. 2008, *Chamaeleon*, ed. Reipurth, B., 169-+
 Luhman, K. L., Allen, L. E., Allen, P. R., et al. 2008, *ApJ*, 675, 1375
 Luhman, K. L., Stauffer, J. R., Muench, A. A., et al. 2003, *ApJ*, 593, 1093
 Luhman, K. L., Wilson, J. C., Brandner, W., et al. 2006, *ApJ*, 649, 894
 Manoj, P., Kim, K. H., Furlan, E., et al. 2011, *ApJS*, 193, 11
 Melo, C. H. F. 2003, *A&A*, 410, 269
 Mugrauer, M., Vogt, N., Neuhäuser, R., & Schmidt, T. O. B. 2010, *A&A*, 523, L1+

- Neuhäuser, R., Brandner, W., Alves, J., Joergens, V., & Comerón, F. 2002, *A&A*, 384, 999
- Neuhäuser, R. & Comeron, F. 1998, *Science*, 282, 83
- Neuhäuser, R., Guenther, E., & Brandner, W. 2003, in *IAU Symposium*, Vol. 211, *Brown Dwarfs*, ed. E. Martín, 309
- Nguyen, D. C., Brandeker, A., van Kerkwijk, M. H., & Jayawardhana, R. 2012, *ApJ*, 745, 119
- Padgett, D. L. & Stapelfeldt, K. R. 2001, in *Bulletin of the American Astronomical Society*, Vol. 33, *Bulletin of the American Astronomical Society*, 1395–+
- Perryman, M. A. C., Lindegren, L., Kovalevsky, J., et al. 1997, *A&A*, 323, L49
- Reipurth, B. & Zinnecker, H. 1993, *A&A*, 278, 81
- Rieke, G. H. & Lebofsky, M. J. 1985, *ApJ*, 288, 618
- Röser, S., Schilbach, E., Schwan, H., et al. 2008, *A&A*, 488, 401
- Rousset, G., Lacombe, F., Puget, P., et al. 2003, in *Presented at the Society of Photo-Optical Instrumentation Engineers (SPIE) Conference*, Vol. 4839, *Adaptive Optical System Technologies II*. Edited by Wizinowich, Peter L.; Bonaccini, Domenico. *Proceedings of the SPIE*, Volume 4839, pp. 140-149 (2003)., ed. P. L. Wizinowich & D. Bonaccini, 140–149
- Schmidt, T. O. B., Neuhäuser, R., Seifahrt, A., et al. 2008a, *A&A*, 491, 311
- Schmidt, T. O. B., Neuhäuser, R., Vogt, N., et al. 2008b, *A&A*, 484, 413
- Siegler, N. 2007, in *In the Spirit of Bernard Lyot: The Direct Detection of Planets and Circumstellar Disks in the 21st Century*, 45
- Skrutskie, M. F., Cutri, R. M., Stiening, R., et al. 2006, *AJ*, 131, 1163
- Stapelfeldt, K. 2001, in *Astronomical Society of the Pacific Conference Series*, Vol. 231, *Tetons 4: Galactic Structure, Stars and the Interstellar Medium*, ed. C. E. Woodward, M. D. Bica, & J. M. Shull, 620–+
- Tetzlaff, N., Neuhäuser, R., & Hohle, M. M. 2011, *MNRAS*, 410, 190
- van Leeuwen, F. 2007, *A&A*, 474, 653
- Vogt, N., Schmidt, T. O. B., Neuhäuser, R., et al. 2012, *A&A*, 546, A63 (Paper I)
- Wenger, M., Oberto, A., Bonnarel, F., et al. 2007, in *Astronomical Society of the Pacific Conference Series*, Vol. 377, *Library and Information Services in Astronomy V*, ed. S. Ricketts, C. Birdie, & E. Isaksson, 197–+
- Zacharias, N., Finch, C., Girard, T., et al. 2010, *AJ*, 139, 2184
- Zacharias, N., Urban, S. E., Zacharias, M. I., et al. 2004, *AJ*, 127, 3043

List of Objects

- ‘HIP 73357’ on page 2
- ‘DI Cha’ on page 3
- ‘Sz 22’ on page 3
- ‘CHXR 32’ on page 3
- ‘ISO-Cha1 144’ on page 3
- ‘HD 97048’ on page 9

Table 5. Absolute astrometric results

Object	JD-2448000 [days]	Ref.	Separation [arcsec] $\rho \pm \delta_\rho$	Sign. ^a	Sign. orb.	PA ^b	Sign. ^a	Sign. orb.	
				not Backg.	motion	[°] $PA \pm \delta_{PA}$	not Backg.	motion	
				$\sigma_{\rho, \text{back}}$	$\sigma_{\rho, \text{orb}}$			$\sigma_{PA, \text{back}}$	$\sigma_{PA, \text{orb}}$
DI Cha AB	5783.85826		4.5444 ± 0.0609	0.5	0.1	202.375 ± 1.236	0.4	0.1	
	5821.80131	1	4.557 ± 0.017	0.4	0.0	202.1 ± 0.6	0.6	0.3	
	6515.62668		4.5510 ± 0.0689	0.2	0.0	202.542 ± 1.400	0.1	0.0	
	6882.64078		4.5556 ± 0.0729	^c	^c	202.559 ± 1.482	^c	^c	
AC	5783.85826		4.6015 ± 0.0616	0.3	0.0	202.062 ± 1.236	0.3	0.0	
	6515.62668		4.6007 ± 0.0696	0.1	0.0	202.136 ± 1.400	0.1	0.0	
	6882.64078		4.5966 ± 0.0735	^c	^c	202.149 ± 1.482	^c	^c	
A(BC) ^d	1476.50000	2	4.9 ± 0.2	0.7	1.5	202 ± 3	0.8	0.3	
	3578.23716	3,4	4.5926 ± 0.0171	1.1	0.2	201.981 ± 0.096	1.2	0.2	
	5783.85826		4.5740 ± 0.0613	0.4	0.0	202.206 ± 1.236	0.3	0.1	
	6515.62668		4.5762 ± 0.0692	0.1	0.0	202.331 ± 1.400	0.1	0.0	
BC	6882.64078		4.5765 ± 0.0732	^c	^c	202.345 ± 1.482	^c	^c	
	5783.85826		0.0623 ± 0.0012	1.8	4.5	178.613 ± 1.661	6.2	6.4	
	5821.80131	1	0.066 ± 0.005	0.8	2.6	177.9 ± 2.3	5.8	5.0	
	6515.62668		0.0593 ± 0.0018	1.0	2.5	169.131 ± 1.579	4.5	2.3	
AD	6882.64078		0.0524 ± 0.0017	^c	^c	163.808 ± 1.629	^c	^c	
	5783.85826		0.2071 ± 0.0038	6.6	0.7	227.326 ± 1.435	4.2	3.1	
	6515.62668		0.2100 ± 0.0046	2.6	0.2	231.638 ± 1.620	1.6	1.0	
Sz 22 AB	6882.64078		0.2105 ± 0.0038	^c	^c	233.890 ± 1.529	^c	^c	
	5783.88427		0.5107 ± 0.0068	3.8	0.5	271.709 ± 1.236	1.1	0.1	
	6515.64511		0.5157 ± 0.0078	^c	^c	271.577 ± 1.402	^c	^c	
CHXR 32 AB	5819.91198	6	2.4372 ± 0.0330	0.9	0.2	285.011 ± 1.244	0.2	0.0	
	6882.90637		2.4471 ± 0.0391	^c	^c	284.924 ± 1.482	^c	^c	
	AC	5819.91198	6	2.3681 ± 0.0345	1.4	0.3	285.311 ± 1.249	0.0	0.2
A(BC) ^d	6882.90637		2.3534 ± 0.0377	^c	^c	285.649 ± 1.482	^c	^c	
	1476.50000	2	2.5 ± 0.5	0.7	0.1	284 ± 5	0.1	0.2	
	4690.70849	5	2.430 ± 0.002	2.8	0.1	285.1 ± 0.5	0.4	0.0	
A(BC) ^e	5819.91198	6	2.4215 ± 0.0329	1.1	0.1	285.077 ± 1.244	0.2	0.0	
	6516.89621		2.4292 ± 0.0369	0.5	0.1	285.103 ± 1.401	0.1	0.0	
	6882.90637		2.4257 ± 0.0388	^c	^c	285.084 ± 1.482	^c	^c	
	5819.91198	6	2.4095 ± 0.0329	1.1	0.0	285.129 ± 1.245	0.1	0.0	
	6882.90637		2.4096 ± 0.0385	^c	^c	285.213 ± 1.482	^c	^c	
BC	5819.91198	6	0.0702 ± 0.0109	0.7	2.5	94.834 ± 2.801	3.1	2.4	
	6882.90637		0.0984 ± 0.0016	^c	^c	87.322 ± 1.497	^c	^c	
Cha H α 5 AB	5782.75127		0.0481 ± 0.0023	1.4	0.6	88.244 ± 4.837	8.4	2.6	
	6881.73805		0.0458 ± 0.0028	^c	^c	111.840 ± 7.758	^c	^c	
Acc1	5782.75127		1.4104 ± 0.0191	0.1	0.8	222.108 ± 1.243	0.9	0.7	
	6881.73805		1.3884 ± 0.0223	^c	^c	220.738 ± 1.483	^c	^c	
Bcc1	5782.75127		1.4442 ± 0.0195	0.3	1.3	223.484 ± 1.240	1.0	0.5	
	6881.73805		1.4040 ± 0.0228	^c	^c	222.508 ± 1.490	^c	^c	
(AB) _{cc1} ^f	5782.75127		1.4272 ± 0.0194	0.1	1.0	222.804 ± 1.244	0.9	0.6	
	6516.68649		1.4103 ± 0.0213	0.1	0.4	222.077 ± 1.400	0.3	0.2	
	6881.73805		1.3963 ± 0.0225	^c	^c	221.619 ± 1.486	^c	^c	

Notes. ^(a) Assuming the fainter component is a non-moving background star. ^(b) Position Angle (PA) is measured from N over E to S. ^(c) Significances are given relative to the last epoch. ^(d) Results of component A relative to the centre of brightness of components B and C. ^(e) Results of component A relative to the centre of mass (masses from apparent magnitudes, Table 9, and distance of Chamaeleon cloud of 165 ± 30 pc, using the models of Baraffe et al. (1998), giving for B $0.76 M_\odot$ and for C $0.28 M_\odot$ at 2 Myr) of components B and C. ^(f) Results of the centre of brightness of components A and B relative to the further companion candidate cc1.

References. (1) Lafrenière et al. (2008). (2) Ghez et al. (1997); date given, assuming midnight for calculation of JD. (3) HST data from ESO/ST-ECF science archive, only position measurement error in RA and Dec considered. (4) From ESO/ST-ECF science archive, see also Stapelfeldt (2001), Padgett & Stapelfeldt (2001). (5) Correia et al. (2006). (6) Rereduced, see also Lafrenière et al. (2008).

Table 6. Relative astrometric results

Object	Epoch difference [days] Δt	Change in separation [pixel] $\Delta \rho \pm \delta_{\Delta \rho}$	Sign. ^{a,c} not Backg. $\sigma_{\rho, \text{back}}$	Sign. ^c orb. motion $\sigma_{\rho, \text{orb}}$	Change in PA ^b [°] $\Delta PA \pm \delta_{\Delta PA}$	Sign. ^{a,c} not Backg. $\sigma_{PA, \text{back}}$	Sign. ^c orb. motion $\sigma_{PA, \text{orb}}$
DI Cha AB	1098.78252	0.846 \pm 0.928	3.3	0.9	0.184 \pm 0.249	2.6	0.7
	367.01410	0.347 \pm 0.379	2.8	0.9	0.017 \pm 0.092	1.9	0.2
AC	1098.78252	-0.365 \pm 0.942	2.0	0.4	0.087 \pm 0.249	2.3	0.3
	367.01410	-0.302 \pm 0.373	1.3	0.8	0.013 \pm 0.091	1.9	0.1
A(BC) ^d	1098.78252	0.187 \pm 0.942	2.6	0.2	0.139 \pm 0.249	2.5	0.6
	367.01410	0.020 \pm 0.389	2.0	0.1	0.014 \pm 0.092	1.9	0.2
BC	1098.78252	-0.743 \pm 0.131	2.0	5.7	-14.805 \pm 1.325	6.9	11
	367.01410	-0.518 \pm 0.163	1.1	3.2	-5.323 \pm 1.001	6.6	5.3
AD	1098.78252	0.256 \pm 0.238	8.5	1.1	6.564 \pm 0.859	7.0	7.6
Sz 22 AB	731.76084	0.374 \pm 0.085	5.2	4.4	-0.132 \pm 0.184	1.6	0.7
CHXR 32 AB	1062.99439	0.746 \pm 0.529	3.3	1.4	-0.087 \pm 0.243	1.0	0.4
	AC	1062.99439	-1.109 \pm 1.092	3.8	1.0	0.338 \pm 0.268	0.1
A(BC) ^d	1062.99439	0.322 \pm 0.557	3.6	0.6	0.007 \pm 0.244	0.8	0.0
	366.01016	-0.260 \pm 0.336	3.8	0.8	-0.019 \pm 0.103	0.8	0.2
A(BC) ^e	1062.99439	0.006 \pm 0.613	3.8	0.0	0.084 \pm 0.246	0.5	0.3
BC	1062.99439	2.130 \pm 0.820	0.7	2.6	-7.512 \pm 2.530	3.2	3.0
Cha H α 5 AB	1098.98678	-0.170 \pm 0.259	1.4	0.7	23.596 \pm 8.940	8.5	2.6
	Acc1	1098.98678	-1.662 \pm 0.395	0.2	4.2	-1.370 \pm 0.295	1.8
Bcc1	1098.98678	-3.037 \pm 0.476	0.4	6.4	-0.976 \pm 0.315	2.1	3.1
(AB)cc1 ^f	1098.98678	-2.333 \pm 0.456	0.1	5.1	-1.185 \pm 0.313	1.9	3.8
	365.05156	-1.055 \pm 0.257	0.5	4.1	-0.458 \pm 0.153	1.7	3.0

Notes. ^(a) Assuming the fainter component is a non-moving background star. ^(b) PA is measured from N over E to S. ^(c) Significances are given relative to the last epoch. ^(d) Results of component A relative to the centre of brightness of components B and C. ^(e) See ^e in Table 5. ^(f) Results of the centre of brightness of components A and B relative to the further companion candidate cc1.

Table 9. Measured brightness differences and mean apparent magnitudes

Object	Epoch	J-band [mag]	H-band [mag]	Ks-band [mag]	Ob- ject	J-band [mag]	H-band [mag]	Ks-band [mag]
DI Cha A(BC)	17 Feb 2006			4.136 \pm 0.010	A	7.841		6.239
	19 Feb 2008	4.232 \pm 0.018		4.347 \pm 0.033	BC	12.073		10.480
	20 Feb 2009 ^b			> 4.104 \pm 0.010	B	12.603		11.077
AB	17 Feb 2006			4.715 \pm 0.007	C	12.749		11.087
	19 Feb 2008	4.770 \pm 0.013		4.980 \pm 0.035	D	12.938 ^a		11.468
	20 Feb 2009 ^b			> 4.737 \pm 0.017				
AC	17 Feb 2006			4.741 \pm 0.007				
	19 Feb 2008	4.919 \pm 0.052		4.974 \pm 0.029				
	20 Feb 2009 ^b			> 4.784 \pm 0.019				
BC	17 Feb 2006			0.026 \pm 0.004				
	19 Feb 2008	0.147 \pm 0.051		-0.006 \pm 0.013				
	20 Feb 2009			0.046 \pm 0.032				
AD	17 Feb 2006			5.298 \pm 0.020				
	19 Feb 2008	5.097 ^a \pm 0.019		5.186 \pm 0.016				
	20 Feb 2009 ^b			> 4.648 \pm 0.006				
Sz 22 AB	17 Feb 2006			3.165 \pm 0.006	A	9.639		6.877
	19 Feb 2008	2.179 \pm 0.007		3.654 \pm 0.014	B	11.818		10.286
CHXR 32 A(BC) ^d	25 Mar 2006 ^c		0.846 \pm 0.008		A		7.599	6.350
	20 Feb 2008			1.940 \pm 0.002	BC		8.445	8.290
AB	25 Mar 2006 ^c			2.150 \pm 0.058	B			8.527
	20 Feb 2009			2.177 \pm 0.005	C			9.843
AC	25 Mar 2006 ^c			3.534 \pm 0.182				
	20 Feb 2009			3.493 \pm 0.006				
BC	25 Mar 2006 ^c			1.384 \pm 0.238				
	20 Feb 2009			1.317 \pm 0.004				
Cha H α 5 AB	16 Feb 2006			0.036 \pm 0.146	A			11.439
	19 Feb 2009			0.153 \pm 0.093	B			11.534
(AB)cc1 ^d	20 Feb 2008			5.234 \pm 0.056	cc1			15.945
Acc1	16 Feb 2006			4.471 \pm 0.070				
	19 Feb 2009			4.469 \pm 0.044				
Acc2	16 Feb 2006			4.458 \pm 0.005				
	19 Feb 2009			4.397 \pm 0.021				

Notes. Mean apparent magnitudes based on combined brightness measurements of 2MASS (Skrutskie et al. 2006). ^(a) Peak to peak brightness difference given. PSF photometry results systematic too low after bad pixel correction in PSF, as bad pixel present despite jittering (only 5 images). ^(b) primary (component A) saturated within this epoch. ^(c) Rereduced, see also Lafrenière et al. (2008). ^(d) PSF photometry does not work in the case of non-resolved (by fitting) double objects, aperture photometry used, see text for further information.